Liquid Crystals
Publication details, including instructions for authors and subscription information:
http://www.informaworld.com/smpp/title~content=t713926090

Thermal behaviour under pressure of the thermotropic cubic mesogen 4'- n -alkoxy-3'-nitrobiphenyl-4-carboxylic acids

Yoji Maeda[a]; Koushi Morita[b]; Shoichi Kutsumizu[b]
[a] Nanotechnology Research Institute, National Institute of Advanced Industrial Science and Technology, Higashi 1-1, Tsukuba, Ibaraki 305-8565, Japan, [b] Department of Chemistry, Faculty of Engineering, Gifu University, Yanagido 1-1, Gifu 501-1193, Japan,

Online publication date: 11 November 2010

To cite this Article Maeda, Yoji , Morita, Koushi and Kutsumizu, Shoichi(2003) 'Thermal behaviour under pressure of the thermotropic cubic mesogen 4'- n -alkoxy-3'-nitrobiphenyl-4-carboxylic acids', Liquid Crystals, 30: 2, 157 — 164
To link to this Article: DOI: 10.1080/0267829031000065164
URL: http://dx.doi.org/10.1080/0267829031000065164

LIQUID CRYSTALS, 2003, VOL. 30, NO. 2, 157–164

Thermal behaviour under pressure of the thermotropic cubic mesogen 4′-*n*-alkoxy-3′-nitrobiphenyl-4-carboxylic acids

YOJI MAEDA*

Nanotechnology Research Institute,
National Institute of Advanced Industrial Science and Technology, Higashi 1-1,
Tsukuba, Ibaraki 305-8565, Japan

KOUSHI MORITA and SHOICHI KUTSUMIZU

Department of Chemistry, Faculty of Engineering, Gifu University, Yanagido 1-1,
Gifu 501-1193, Japan

(*Received 22 July 2002; in final form 26 September 2002; accepted 12 October 2002*)

The thermal behaviour of members of a homologous series which exhibits the optically isotropic cubic phase, the 4′-*n*-alkoxy-3′-nitrobiphenyl-4-carboxylic acids having alkoxy chains containing 16, 20 and 22 carbon atoms (referred to as ANBC-16, -20 and -22, respectively) was investigated under pressures up to 200–400 MPa by high pressure differential thermal analysis. In the phase diagram of ANBC-16 obtained on heating, a triple point was estimated at 54 ± 1 MPa and 205 ± 1°C for the SmC, Cub and SmA phases. It was found that the X phase is formed on cooling under all pressures, while appearing on heating at high pressures above about 54 MPa. Thus the X phase appears monotropically between the SmA and Cub phases in the low pressure region and enantiotropically between the SmA and SmC phases under higher pressures. It is strongly suggested that the X phase is a columnar mesophase. For ANBC-20 and -22, the cubic phase tends to be destabilized with increasing pressure. The temperature region of the cubic phase of ANBC-20 becomes narrower with increasing pressure and a triple point for the SmC, Cub and I phases is estimated to be at about 309 MPa. On the other hand, the cubic phase of ANBC-22 is still observed at the highest pressure examined.

1. Introduction

In 1957 Gray *et al.* [1] reported the synthesis of a homologous series of mesomorphic 4′-*n*-alkoxy-3′-nitrobiphenyl-4-carboxylic acids, ANBC-*n*, where *n* is the number of carbon atoms in the alkoxy chain (see structure below). The polymorphism of the hexadecyloxy and octadecyloxy derivatives was investigated by Demus *et al.* [2]. They found a new optically isotropic mesophase, which was classified as the smectic D phase, between the smectic C (SmC) phase and the smectic A (SmA) or isotropic (I) phases. Since then, increasing attention has focused on the structure and thermal stability of this phase [3–5] which is now called the cubic phase because a layered smectic structure is inconsistent with the observed optical isotropic properties.

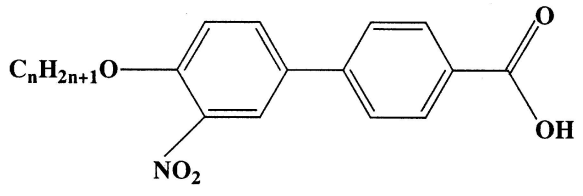

*Author for correspondence; e-mail: yoji.maeda@aist.go.jp

The thermotropic cubic phase shown by the ANBC-*n* homologues is one of the most fascinating phases in the field of liquid crystalline systems in that some types of rod-like molecules form an optically isotropic structure in a temperature range sandwiched by other anisotropic phases with lamellar, hexagonal, or columnar structures [6]. The stability of the cubic phase for the ANBC-*n* series is strongly dependent upon the length *n* of the alkoxy groups, as shown in figure 1. The ANBC-*n* homologues show the cubic phase for $n \geqslant 15$ (and up to 26 at present) and over a temperature region which becomes broader, essentially, with increasing *n* [5].

In the solid and liquid crystalline phases, most of the ANBC-16 molecules are dimerized via intermolecular hydrogen bonds [7, 8], and thus the structural unit is the dimerized molecule that has an extended core of coupled nitrobiphenylcarboxylic acids at its centre and two terminal alkoxy chains. Tardieu and Billard [9] identified the space group *Ia3d* for the cubic phase of ANBC-16, and showed that the unit cell contains about 1000 molecules of ANBC-16. They adopted the interwoven jointed-rod model, which was first postulated for

Liquid Crystals ISSN 0267-8292 print/ISSN 1366-5855 online © 2003 Taylor & Francis Ltd
http://www.tandf.co.uk/journals
DOI: 10.1080/0267829031000065164

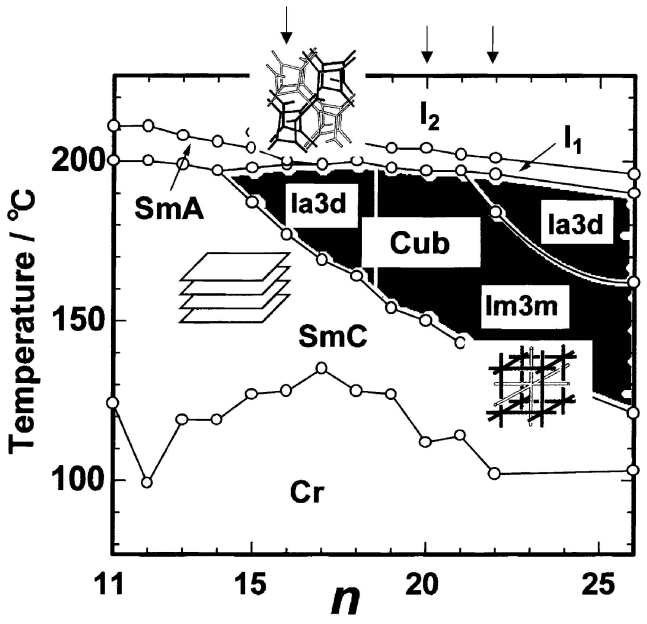

Figure 1. Phase behaviour as a function of the number of carbon atoms *n* in the alkoxy group for the ANBC-*n* series. Cr, crystal; SmC/A, smectic C/A; Cub, cubic; I_1, 'structured liquid'; I_2, isotropic liquid.

the lyotropic *Ia3d* cubic phases by Luzzati and Spegt [10]. The model has been supported by other researchers using X-ray diffraction (XRD) [11, 12], NMR spectroscopic [13], and dynamic viscoelastic techniques [14]. Precise calorimetric measurements were also carried out, providing reliable thermodynamic quantities for the phase transitions involving cubic phases [15–18].

Shankar Rao *et al.* constructed an interesting *T* vs. *P* phase diagram of ANBC-16 using transmitted light intensity measurements on cooling under pressure [19]: the cubic phase disappears at about 40 MPa, while a columnar (Col) phase is formed between the SmA and SmC (or Cub) phases over the whole pressure region studied. We also studied the thermal behaviour of ANBC-16 using high pressure differential thermal analysis (DTA) and determined the *T* vs. *P* phase diagram on heating; this exhibits a triple point indicating the upper limit for the cubic phase [20]. The *T* vs. *P* phase diagram is clearly different from the phase diagram reported by Shankar-Rao *et al.* and particularly with respect to the triple point. This difference in *T* vs. *P* phase diagrams prompted us to investigate the thermal behaviour of a homologous series of ANBC-*n* compounds under hydrostatic pressure, with particular focus on the effect of pressure on the phase stability of the cubic phase.

In this paper, we present the experimental results of the thermal behaviour of a homologous series of ANBC-*n* compounds having different alkoxy chain lengths, ANBC-16, -20, and -22, under hydrostatic pressures up to 200–400 MPa by high pressure DTA measurements.

2. Experimental

2.1. *Sample preparation*

The ANBC-*n* compounds were prepared according to the method described by Gray *et al.* [1]. Samples were recrystallized from ethanol several times and the purity was confirmed by infrared (IR), ^{1}H NMR, and mass spectroscopies (MS), and by elemental analysis.

2.2. *DSC measurements*

The ANBC-*n* compounds were characterized by differential scanning calorimetry (DSC) and polarizing optical microscopy (POM) under atmospheric pressure. Thermal characterization was performed on a Perkin-Elmer DSC-7 and Seiko Instruments SSC-5000 calorimeters at a scanning rate of 5°C min^{-1} under N_2 gas flow. Temperatures and heats of transition were calibrated using the standard materials, namely, indium and tin. Transition temperatures were determined as the onset of the transition peaks, i.e. the temperature at which the tangential line of the inflection point of the rising part of the peak intersects the extrapolated baseline. By contrast, the I_1–I_2 transition point was assigned as the peak temperature because the I_1–I_2 transition overlaps with the peak associated with either the SmA–I_1 transition for ANBC-16 or the Cubic–I_1 transition for ANBC-20 and -22.

2.3. *DTA measurements under pressure*

The high pressure DTA apparatus used in this study is described elsewhere [21]. The DTA system was operated between room temperature and 250°C under hydrostatic pressures up to 500 MPa. Dimethylsilicone oil with a medium viscosity (100 cSt) was used as the pressurizing medium. The sample weighing about 4 mg was put in the sample cell and coated with epoxy adhesives, both to fix the sample in the cell and also to prevent direct contact with the silicone oil. The DTA runs were performed at a constant scanning rate of 5°C min^{-1} under various pressures. Transition temperatures were determined in the same manner as in the DSC analysis. Since ANBC-*n* compounds were of low stability, a virgin sample was used for each DTA measurement.

3. Results and discussion

3.1. *ANBC-16*

The thermal characterization of ANBC-16 and ANBC-18 has already been reported; the transition sequence is $Cr \leftrightarrow SmC \leftrightarrow Cub \leftrightarrow SmA \leftrightarrow I_1 \leftrightarrow I_2$ for ANBC-16 and

$Cr \leftrightarrow SmC \leftrightarrow Cub \leftrightarrow I_1 \leftrightarrow I_2$ for ANBC-18 at atmospheric pressure [2–5]. The I_1–I_2 transition is assigned to the dissociation of hydrogen-bonded dimers between the terminal carboxylic acid groups [5–7]. It is reported that a monotropic mesophase often appears between the SmA and Cub phases on slow cooling [3, 19], and this has been suggested to be either a tetragonal [12] or a columnar phase [22]. Figure 2 shows the DSC heating and cooling curves of ANBC-16 at a scanning rate of $5^{\circ}C\ min^{-1}$. As already reported, a very metastable mesophase is observed monotropically over a small temperature interval of 1–2°C between the SmA and Cub phases on cooling. Thus the transition sequence is $I_2 \rightarrow I_1 \rightarrow$ SmA → monotropic mesophase → Cub → SmC → Cr_1 on cooling.

We re-examined the thermal behaviour of ANBC-16 on heating and subsequent cooling under hydrostatic pressures up to 150 MPa using DTA, to examine the behaviour under various pressures, of the unknown X phase which appears on heating under high pressure above about 60 MPa [20]. If the transition behaviour under pressure is measured continuously from atmospheric to high pressures, it can be understood as a function of pressure. However, it was difficult to obtain clear DTA curves for ANBC-16 on cooling from the I_2 phase under pressure because the DTA baseline drifted significantly in the cooling process, and especially at low pressures. Another difficulty was due to the sample itself because the $I_2 \rightarrow I_1$ transition often occurs incompletely on cooling and this is shown in repeated DSC measurements of the sample. Thus we performed the DTA cooling measurements of ANBC-16 by cooling from a temperature in the I_1 phase, in order to reduce the dissociation of the dimerized molecules (i.e. I_1–I_2 transition) as much as possible. Figure 3 shows the DTA heating and subsequent cooling curves of ANBC-16 at 27 MPa. As reported in the preceding paper [20], the $Cr_1 \rightarrow$ SmC → Cub → SmA → I_1 transition sequence was confirmed on heating at 27 MPa. On cooling the significant drift in the baseline was observed as an undulation, but none the less small transition peaks can be seen on the DTA curve. We see three small exothermic peaks, attributable to the SmA → X, X → Cub, and Cub → SmC transitions, in order of decreasing temperature. The large peak and finally a small peak at the lowest temperatures were assigned to SmC → Cr_1 and $Cr_1 \rightarrow Cr_4$ transitions, respectively. The temperature range of the SmA phase was considerably broader on cooling than on heating. Thus, the transition sequence $I_1 \rightarrow$ SmA → X → Cub → SmC → $Cr_1 \rightarrow Cr_4$ was detected on cooling at 27 MPa. It is noted that the X phase appears monotropically between the SmA and Cub phases under low pressures and so the phase is metastable.

Figure 4 shows the DTA heating and subsequent cooling curves of ANBC-16 at 100 MPa. As reported earlier, the transition sequence $Cr_4 \rightarrow Cr_1 \rightarrow$ SmC → X → SmA → I_1 is observed on heating. The X phase appears in place of the cubic phase in the high pressure region. The subsequent cooling curve exhibits completely the reverse process. Hence it can be said that the X phase appears enantiotropically between the SmA and SmC phases at 100 MPa.

In the phase diagram constructed on heating, the temperature region of the optically isotropic cubic phase becomes narrower with increasing pressure, and disappears at high pressures above about 60 MPa. We understood that the phase sequence on heating changes from SmC → Cub → SmA → I_1 at atmospheric pressure to SmC → X → SmA → I_1 in the high pressure region,

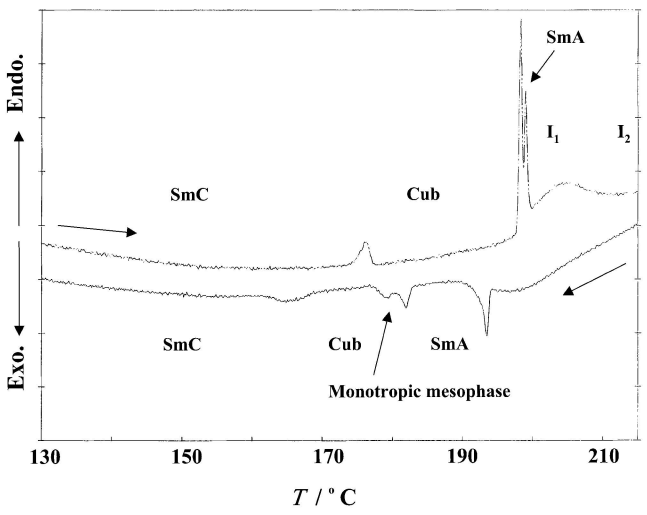

Figure 2. DSC curves of ANBC-16 at a scanning rate of $5^{\circ}C\ min^{-1}$.

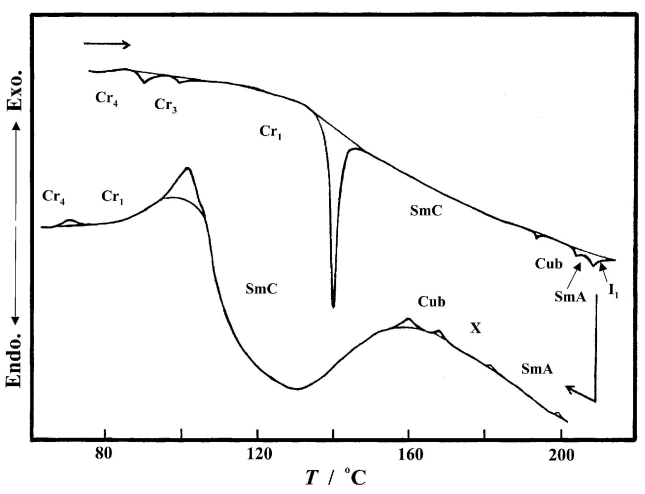

Figure 3. DTA heating and cooling curves of ANBC-16 at 27 MPa. Scanning rate: $5^{\circ}C\ min^{-1}$.

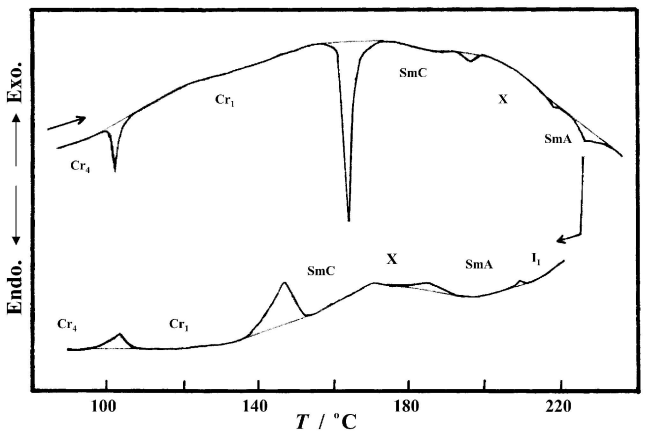

Figure 4. DTA heating and cooling curves of ANBC-16 at 100 MPa. Scanning rate: 5°C min^{-1}.

via SmC → (X) → Cub → SmA → I_1 in the low pressure region. The X phase was supposed to appear between the SmC and Cub phases in the low pressure region although the SmC–X transition could not be observed clearly on heating. This supposition is in contradiction, however, with the experimental data. Hence we now consider the transition sequence to involve the X phase in the low pressure region; the SmC → Cub → SmA → I_1 sequence is held at pressures up to 54 MPa.

Figure 5 shows the T vs. P phase diagram for ANBC-16 obtained both on heating [20] and cooling.

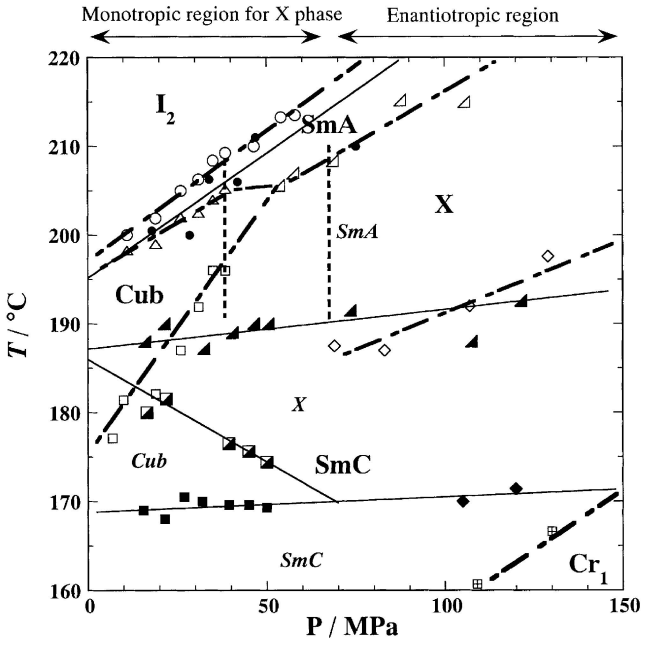

Figure 5. T vs. P phase diagrams of ANBC-16 constructed on cooling and heating. Thin solid lines and filled symbols are for the T vs. P diagram constructed on cooling, while dotted, bold lines and open symbols are for the phase diagram obtained on heating.

Focusing on the phase behaviour of the cubic and X phases on heating, the Cub–SmA transition line in the low pressure region below 40 MPa is a little displaced from the X–SmA transition line in the high pressure region above 55 MPa, and there is a boundary region over 40–70 MPa between the two phase regions, as shown by the dotted vertical lines in figure 5. Strictly speaking, the structural behaviour is still not clear in the boundary region. In the preceding paper we reported the triple point (65 MPa and 207.6°C) for the X, Cub and SmA phases, which was obtained by linear extrapolation of the SmC–Cub and Cub (or X)–SmA transition curves. In this study, the triple point was reevaluated to be at 54 ± 1 MPa and at 205 ± 1°C for the SmC, Cub and SmA phases.

The transition curves obtained on heating and cooling can be expressed approximately as first or second order polynomials in terms of pressure as follows:

Heating mode

$0 \leqq P \leqq 40$ MPa

SmC → Cub	$T = 172.9 + 0.591_0 P$
Cub → SmA	$T = 195.0 + 0.258_5 P$

$55 \leqq P \leqq 100$ MPa

SmC → X	$T = 172.8 + 0.179_4 P$
X → SmA	$T = 191.6 + 0.248_6 P$

Whole pressure range

Cr_1 → SmC transition	$T = 125.9 + 0.350_2 P - 2.77_4 \times 10^{-4} P^2$
SmA → I.	$T = 198.4 + 0.248_2 P$

Cooling mode

$0 \leqq P \leqq 70$ MPa

X → Cub	$T = 183.8 - 0.176_3 P$
Cub → SmC	$T = 168.3 + 0.027_5 P$

Whole pressure range

I. → SmA	$T = 197.3 + 0.197_1 P$
SmA → X	$T = 187.6 + 0.029_7 P$
SmC → Cr_1	$T = 103.7 + 0.375_8 P$

An important feature of the phase diagram constructed in the cooling mode is the appearance of the X phase over the whole pressure region. The enantiotropic X phase between the SmA and SmC phases has a temperature width of about 20° in the high pressure region, while the temperature range of the monotropic X phase decreases with decreasing pressure, due to the appearance of the cubic phase. It should be noted that the X → Cub transition line has a strong negative slope ($dT/dP \fallingdotseq -17$°C/100 MPa) with pressure, while all the other transition lines have positive slopes, as already reported by Shankar Rao *et al.* [19]. Furthermore, figure 5 suggests the strong possibility that the monotropic X phase may appear at atmospheric pressure, as deduced by extrapolating both the SmA–X and X–Cub transition lines to the ordinate. This possibility is supported by the appearance of a monotropic mesophase

on cooling at atmospheric pressure, as shown in figure 2. Thus the X phase corresponds to the monotropic mesophase having either a columnar or tetragonal structure as previously reported [3, 12, 19, 22]. The T vs. P phase diagram made on cooling is similar to the phase diagram reported by Shankar-Rao *et al*., although the transition curves are considerably different: the Col–Cub boundary showed a negative slope, $(dT/dP)_{1atm} = -10.9°C/100\,MPa$, and also a triple point appeared at about 40 MPa for the Col, Cub and SmC phases. In figure 5, the X–Cub transition line has a strong negative slope and merges with the Cub–SmC transition line at about 70 MPa, leading to a triple point for the X, Cub and SmC phases. We should note, however, that the monotropic X phase is not thermodynamically stable.

3.2. *ANBC-20 and -22*

Figure 6 shows the DSC heating curves of ANBC-20 and -22. Both samples exhibit the transition sequence $Cr \rightarrow SmC \rightarrow Cub \rightarrow I_1 \rightarrow I_2$ [4, 5]. The DSC curves show a main peak associated with the Cr–SmC transition, two smaller peaks corresponding to the SmC–Cub and Cub–I_1 transitions at higher temperatures, and finally a broad peak associated with the I_1–I_2 transition. Transition temperatures and associated enthalpy changes are listed in the table. According to XRD [23–25], the cubic structure for ANBC-16 belongs to the *Ia*3*d* space group, while that for ANBC-20 belongs to the *Im*3*m* space group. ANBC-22 has two types of cubic structure with the *Im*3*m* and *Ia*3*d* space groups. Unfortunately the Cub(*Im*3*m*)–Cub(*Ia*3*d*) transition is too small to be detected by the conventional DSC technique. Recently the transition was detected using a high precision adiabatic calorimeter by Saito *et al.* [26]. Thus the actual transition sequences for ANBC-20 and -22 on heating are Cr–SmC–Cub(*Im*3*m*)–I_1–I_2 and Cr–SmC–Cub(*Im*3*m*)–Cub(*Ia*3*d*)–I_1–I_2, respectively. It is interesting to study the effect of pressure on the thermal behaviour of these compounds because they have cubic phases with different space groups.

Figure 7 shows the DTA heating curves of ANBC-20 in the pressure region up to 200 MPa. All the endothermic peaks associated with the transitions low-temperature crystal form (Cr_2) → high temperature one (Cr_1), $Cr_1 \rightarrow SmC$, $SmC \rightarrow Cub$, and $Cub \rightarrow I_1$ were clearly detected at pressures up to 100 MPa. The SmC–Cub transition peak became very small at 150 and 200 MPa. Compared with ANBC-16, the destabilization of the cubic phase in ANBC-20 occurs slowly with increasing pressure. Figure 8 shows the T vs. P phase diagram of ANBC-20 in the pressure region up to 300 MPa. The transition curves for ANBC-20 constructed on heating can be expressed approximately as first order polynomials in terms of pressure as follows:

Whole pressure range

$Cr_2 \rightarrow Cr_1$ transition	$T = 78.7 + 0.100_4 P$
$Cr_1 \rightarrow SmC$	$T = 112.3 + 0.280_5 P$
$SmC \rightarrow Cub$	$T = 149.4 + 0.338_3 P$
$Cub \rightarrow I_1$	$T = 192.5 + 0.198_6 P$

Figure 8 suggests that the SmC–Cub transition line with the higher slope ($dT/dP = 33.8°C/100\,MPa$) will merge with the Cub–I_1 transition line at high pressure. The triple point for the SmC, Cub(*Im*3*m*) and I_1 phases is expected to be at 309 MPa and 254°C.

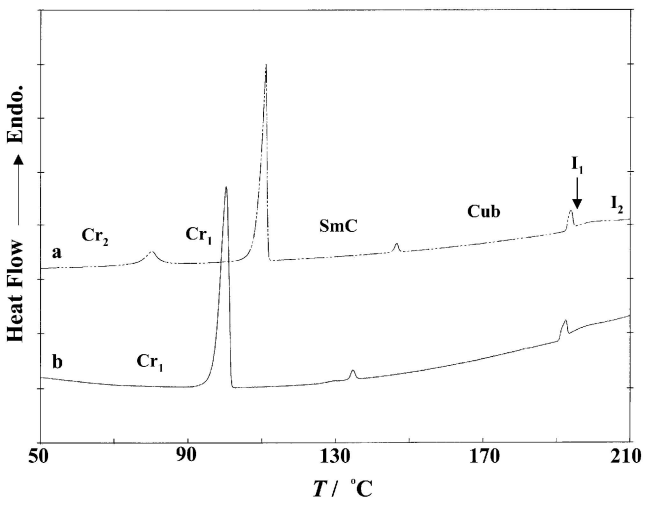

Figure 6. DSC heating curves of ANBC-20 and -22 at a heating rate of 5°C min^{-1}: (*a*) ANBC-20, (*b*) ANBC-22.

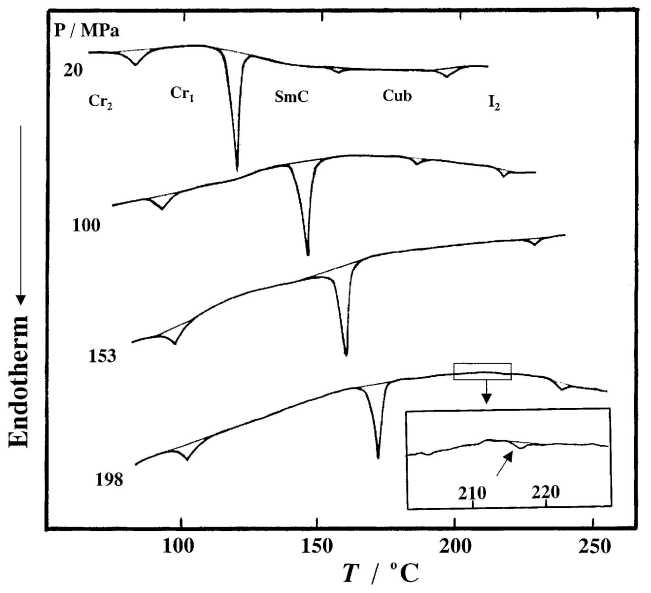

Figure 7. DTA heating curves of ANBC-20 under various pressures. Heating rate: 5°C min^{-1}.

Table. Thermodynamic quantities associated with the phase transitions on heating for a homologous series of ANBC-*n* compounds with $n = 16$, 20 and 22 at atmospheric pressure. Upper figure is temperature (°C); lower figures is enthalpy (kJ mol^{-1}).

Sample	Cr_4–Cr_3	Cr_3–Cr_2	Cr_2–Cr_1	Cr_1–SmC	SmC–Cub	Cub–SmA	SmA–I_1
ANBC-16							
	47.5	74.5	89.4	125.0	174.5	197.9	198.8
	0.6	2.3	0.2	38.6	0.5	1.5	0.9
						Cub–X X–SmA	
	cooling			86.7	165.6	179.9 182.8	193.9
				32.3	0.4	0.75	0.7
ANBC-20							
			76.9	108.8	145.5	192.6	
			6.9	44.7	1.3	2.7	
ANBC-22							
				97.2	133.6	190.8	
				29.5	0.6	1.2	

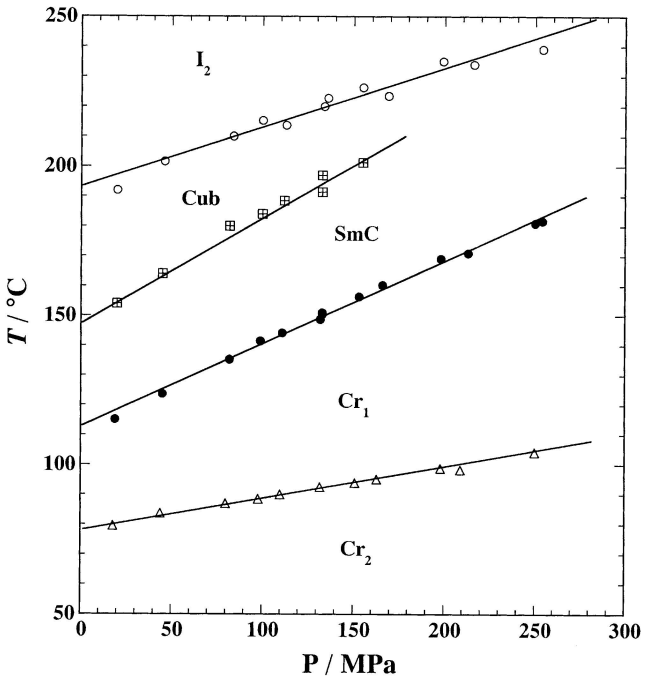

Figure 8. *T* vs. *P* phase diagram of ANBC-20 constructed on heating.

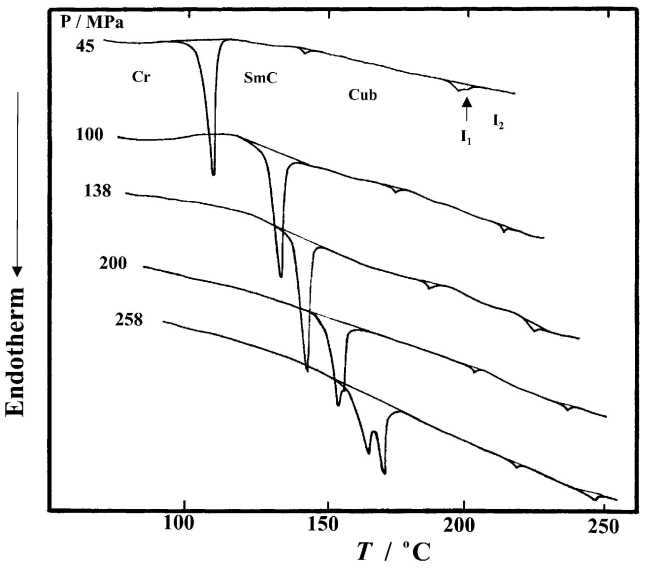

Figure 9. DTA heating curves of ANBC-22 under various pressures. Heating rate: 5°C min^{-1}.

As we have noted, ANBC-22 has two kinds of cubic phases with *Im*3*m* and *Ia*3*d* space groups in the low and high temperature regions, respectively [23–25]. The thermal behaviour of ANBC-22 was measured under hydrostatic pressures up to 400 MPa. Figure 9 shows the DTA heating curves of ANBC-22 in the pressure region up to 260 MPa. ANBC-22 apparently showed the same transition sequence Cr → SmC → Cub → I_1 → I_2 as ANBC-20 because the Cub(*Im*2*m*)–Cub(*Ia*3*d*) transition could not be observed at any pressure. On the other hand, the main peak associated with the Cr–SmC transition splits into a double peak at high pressures above 160 MPa. This phenomenon indicates the formation of a pressure-induced crystalline polymorph, denoted here as Cr_i. The Cr → Cr_i → SmC → Cub → I_1 transition sequence was observed in the high pressure region up to 400 MPa. Figure 10 shows the *T* vs. *P* phase diagram of ANBC-22 in the pressure range up to 400 MPa. It is noted that the change in slope of the SmC–Cub transition line occurs at about 160 MPa and at the same time the Cr_i polymorph appears between the Cr and SmC phases. The cubic phase remains at 400 MPa. The transition curves can be expressed approximately as first order polynomials of pressure as follows.

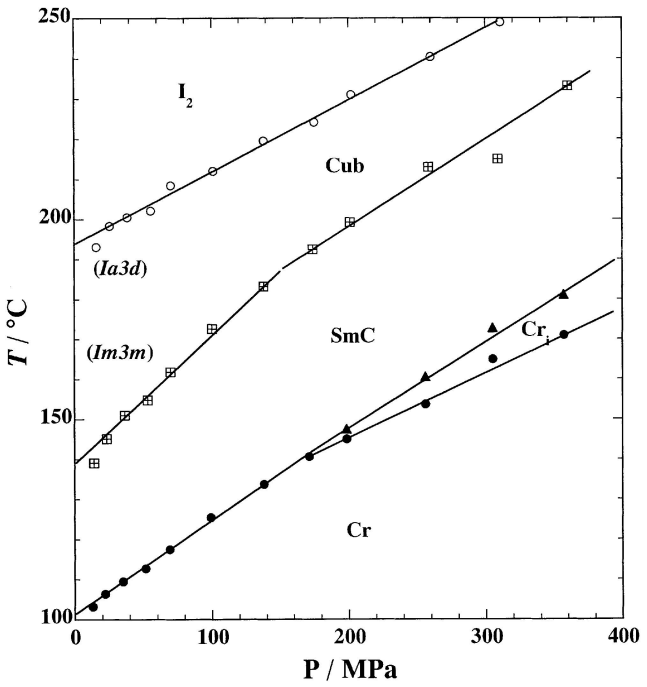

Figure 10. T vs. P phase diagram of ANBC-22 constructed on heating.

$0 \leqq P \leqq$ c. 160 MPa

Cr → SmC transition	$T = 101.0 + 0.236_2 P$
SmC → Cub	$T = 137.5 + 0.328_1 P$

c. 160 MPa < P

Cr → Cr_i	$T = 118.4 + 0.142_3 P$
Cr_i → SmC	$T = 112.1 + 0.189_6 P$
SmC → Cub	$T = 156.1 + 0.209_9 P$

Whole pressure range

Cub → I_1	$T = 193.1 + 0.182_9 P$

The cubic phase is destabilized with increasing pressure but this destabilization is stopped in the high pressure region up to 400 MPa. The change in slope of the SmC–Cub transition line may indicate that the low temperature cubic phase disappears at about 160 MPa while the other cubic phase remains in the high pressure region. Unfortunately we can not further discuss the phase stability of the cubic phases because the Cub(*Im*3*m*)–Cub(*Ia*3*d*) transition could not be detected in this study.

4. Conclusion

Based on the results of this study, the cubic phases of the ANBC-*n* homologues are destabilized with increasing pressure although its temperature interval tends to increase on extending the alkoxy chain length *n* from 16 to 22. The cubic phases of ANBC-16 and -20 finally disappear at about 54 and 309 MPa, respectively, while the cubic phase of ANBC-22 remains at the highest pressure examined.

Concerning the highly metastable X phase seen for ANBC-16, it was confirmed that this appears monotropically between the SmA and Cub phases in the low pressure region below 54 MPa, and enantiotropically between the SmA and SmC phases in the high pressure region. The transition sequence for ANBC-16 is, in the low pressure region below 54 MPa,

$$Cr_1 \rightleftharpoons SmC \rightleftharpoons Cubic \begin{array}{c} \longrightarrow \\ \nwarrow X \swarrow \end{array} SmA \rightleftharpoons I_1 \rightleftharpoons I_2$$

and in the high pressure region,

$$Cr_1 \rightleftharpoons SmC \rightleftharpoons X \rightleftharpoons SmA \rightleftharpoons I_1 \rightleftharpoons I_2$$

The monotropic X phase in the low pressure region appears to be related to the mesophase observed between the SmA and Cub phases on cooling at atmospheric pressure, and is suggested to be either a columnar [21] or a tetragonal phase [12]. The structure of the X phase is not clear, but very recently has been found to exhibit a plate-like fan texture or a sanded texture similar to that of the SmC phase under pressure, and shows a spot-like WAXD pattern, suggesting it is not a layered structure [27]. Thus there is a strong suggestion that the X phase is a columnar hexagonal phase.

The transition sequence $Cr_1 \leftrightarrow SmC \leftrightarrow Cub \leftrightarrow I_1 \leftrightarrow I_2$ is common to both ANBC-20 and -22 over a wide pressure region. For ANBC-20 the cubic phase is expected to disappear at about 309 MPa, while for ANBC-22 the cubic phase remains, even at 400 MPa. Structural investigations are needed to obtain a better understanding of the cubic phase under pressure; those are now in progress in our research group.

We would like to express sincere thanks to Prof. Shinichi Yano of Gifu University for encouraging this research. S.K. acknowledges financial support of the Ministry of Education, Science, Sports, Culture, and Technology in Japan (Grant-in-Aid for Scientific Research on Priority Areas (A), No. 413/13031037 and 14045232 and Grant-in-Aid 14550846).

References

[1] Gray, G. W., Jones, B., and Marson, F., 1957, *J. chem. Soc*., 393.
[2] Demus, D., Kunicke, G., Neelsen, J., and Sackmann, H., 1968, *Z. Naturforsch*., **23a,** 84.
[3] Demus, D., Marzotko, D., Sharma, N. K., and Wiegeleben, A., 1980, *Krist. Tech*., **15,** 331.
[4] Gray, G. W., and Goodby, J. W., 1984, *Smectic Liquid Crystals—Textures and Structures* (Glasgow: Leonard Hill), Chap. 4.

[5] Kutsumizu, S., Yamada, M., and Yano, S., 1994, *Liq. Cryst*., **16,** 1109.
[6] Diele, S., and Göring, P., 1998, *Handbook of Liquid Crystals*, Vol. 2B, edited by D. Demus, J. Goodby, G. W. Gray, H.-W. Spiess, and V. Vill (Weinheim: Wiley-VCH), pp. 887–900.
[7] Kutsumizu, S., Kato, R., Yamada, M., and Yano, S., 1997, *J. phys. Chem. B*, **101,** 1666.
[8] Tansho, M., Onoda, Y., Kato, R., Kutsumizu, S., and Yano, S., 1998, *Liq. Cryst*., **24,** 525.
[9] Tardieu, A., and Billard, J., 1976, *J. Phys. (Paris) Coll*., **37,** C3-79.
[10] Luzzati, V., and Spegt, A., 1967, *Nature*, **215,** 701.
[11] Levelut, A.-M., and Fang, Y., 1991, *Colloq. Phys*., **23,** C7-229.
[12] Levelut, A.-M., and Clerc, M., 1998, *Liq. Cryst*., **24,** 105.
[13] Ukleja, P., Siatkowski, R. E., and Neubert, M., 1988, *Phys. Rev. A*, **38,** 4815.
[14] Yamaguchi, T., Yamada, M., Kutsumizu, S., and Yano, S., 1995, *Chem. Phys. Lett*., **240,** 105.
[15] Saito, K., Sato, A., and Sorai, M., 1998, *Liq. Cryst*., **25,** 525.
[16] Morimoto, N., Saito, K., Morita, Y., Nakasuji, K., and Sorai, M., 1999, *Liq. Cryst*., **26,** 219.
[17] Sato, A., Saito, K., and Sorai, M., 1999, *Liq. Cryst*., **26,** 341.
[18] Sato, A., Yamamura, Y., Saito, K., and Sorai, M., 1999, *Liq. Cryst*., **26,** 1185.
[19] Shankar Rao, D. S., Krishna Prasad, S., Prasad, V., and Kumar, S., 1999, *Phys. Rev. E*, **59,** 5572.
[20] Maeda, Y., Cheng, G.-P., Kutsumizu, S., and Yano, S., 2001, *Liq. Cryst*., **28,** 1785.
[21] Maeda, Y., and Kanetsuna, H., 1985, *Bull. Res. Inst. Polym. Tex*., **149,** 119; Maeda, Y., 1990, *Thermochim. Acta*., **163,** 211.
[22] Lydon, J. E., 1981, *Mol. Cryst. liq. Cryst. Lett*., **72,** 79.
[23] Kutsumizu, S., Ichikawa, T., Nojima, S., and Yano, S., 1999, *Chem. Commun*., 1181.
[24] Kutsumizu, S., Ichikawa, T., Yamada, M., Nojima, S., and Yano, S., 2000, *J. Phys. Chem. B*, **104,** 10 196.
[25] Kutsumizu, S., Morita, K., Ichikawa, T., Yano, S., Nojima, S., and Yamaguchi, T., *Liq. Cryst*. (in the press).
[26] Saito, K., Shinhara, T., Nakamoto, T., Kutsumizu, S., Yano, S., and Sorai, M., 2002, *Phys. Rev. E*, **65,** 031719.
[27] Maeda, Y., Prasad, S. K., Kutsumizu, S., and Yano, S. (to be published).